2206

MORPHOLOGY AND MECHANICAL PROPERTIES OF LAYERED SILICATE REINFORCED NATURAL (NR) AND POLYURETHANE (PUR) RUBBER BLENDS PRODUCED BY LATEX COMPOUNDING

Dr Siby Varghese, Scientist (Rubber Technology)
Rubber Technology Division, Rubber research Institute of India, Kottayam, Kerala 686009,
Email: sibyvarghese100@yahoo.com

BIOGRAPHICAL NOTE

Dr. Siby Varghese is a scientist of Rubber Research Institute of India and he received his doctorate in 1992. He did his postdoctoral research (1996 to 1998) under the JSPS (Japan Society for Promotion of Science) postdoctoral programme at University of Tokyo, Japan in the area of radiation processing of polymers. For his scientific contributions he has received the Indian Young Scientist Award in 1996. His responsibilities include designing and leading of polymer projects of popular interest, trouble shooting of factory processes, conducting training programs for polymer students and entrepreneurs, supervision of students for PhD programme etc. In 2002, he has been selected for the famous AvH (Alexander von Humboldt) post-doctoral fellowship at Institute for Composite Materials (IVW), University of Kaiserslautern, Germany. He has 70 international publications and conducted several presentations in international level. He has 6 patents in his credit. His specific area of research interest includes polymer composites, blends, rubber nanocomposites, latex allergy, recycling etc.

ABSTRACT

Natural rubber (NR), polyurethane rubber (PUR) and NR/PUR-based nanocomposites were produced from the related latices by adding a pristine synthetic layered silicate (LS; sodium fluorohectorite) in 10 parts per hundred parts rubber (phr). The dispersion of the LS latices in the composite was studied by X-ray diffraction (XRD) and transmission electron microscopy (TEM). Further information on the rubber/LS interaction was received from Fourier transform infrared spectroscopy (FTIR) and dynamic mechanical thermal analysis (DMTA). Tensile and tear tests were used to characterise the performance of the rubber nanocomposites. It was found that LS is more compatible and thus better intercalated by PUR than by NR. Further, LS was preferably located in the PUR phase in the blends which exhibited excellent mechanical properties in spite of the uncompatibility between NR and PUR. Nanoreinforcement was best reflected in stiffness- and strength-related properties of the rubber composites.

INTRODUCTION

Nowadays rubber nanocomposites containing layered silicates (LS) as reinforcement are gaining importance [1]. The interest behind this development is due to the nanoscale dispersion (the thickness of the layered silicates is ca. 1nm) and very high aspect ratio of the silicate platelets (length to thickness ratio is up to 2000) [2] enabling high reinforcing efficiency even at low LS loading. In order to make the polar LS compatible with nonpolar polymers and thus to facilitate the exfoliation of LS, the silicates are made organophilic [e.g. [2-3]. This occurs by exploiting the cation exchange capacity of the LS. Organophilic LS are, however expensive which forced the researchers to have a look at alternative methods. Non-organophilic (pristine) LS can be dispersed in water which acts as swelling agent via hydration of the intergallery cations (usually Na^+ ions). Note that several rubbers are available in latex form which is rather stable aqueous dispersion of fine rubber particles (particle size usually below 5 μm). Mixing of latex with LS followed by coagulation is therefore an interesting way to produce rubber nanocomposites. This route has been already followed for natural (NR) [4], styrene/butadiene (SBR) [5-6], acrylonitrile/butadiene (NBR) [7] and carboxylated NBR [8]. On the other hand, no report is available on LS-reinforced latex blends. This is quite surprising as latex combinations are widely used to improve some praxis-relevant properties of the constituents. Note that NR has to be filled/reinforced owing to its moderate tear strength [e.g. 9-10]. In order to improve the resistance to solvents (specially towards hydrocarbons), to abrasion and to UV-irradiation, NR is often blended with polyurethane rubber (PUR). Accordingly, the aims of its present work were a) to produce LS-reinforced NR/PUR-based nanocomposites via latex compounding, and b) to study their morphology-dependent mechanical properties.

EXPERIMENTAL

Materials. As LS a synthetic sodium fluorohectorite (Somasif ME-100) of Co-op Chemicals (Tokyo, Japan) was selected. This LS had a cation exchange capacity of 100meq/100g and an intergallery distance of 0.95nm. Note that this LS exhibits a very high aspect ratio, viz.>1000 [4, 11].

Sulfur prevulcanized NR latex was procured from Rubber Research Institute of India (Kerala, India). This concentrated, high-ammonia (1%) NR latex contained 60% dry rubber. For prevulcanization this latex was mixed with the ingredients listed in Table 1 with slow stirring. The compounded latex was then heated to 70°C in a water bath with low stirring for 4h. The prevulcanized latex that obtained was cooled to room temperature and the initial ammonia content was restored by adding ammonia solution. The NR latex was then stored in tight plastic bottles until use.

PUR latex (Impranil DLP-R) containing ca. 50% polyester-based polyurethane was supplied by Bayer (Leverkusen, Germany).

Film casting. The prevulcanized NR latex was mixed with the aqueous dispersion of LS (10%) and stirred well. The dirt and coarse particles were removed by filtering through a sieve (opening 250μm) and the latex compound was cast in a mold build of glass plates (dimensions: 130mm x 100mm x 2mm). The casting was allowed to dry in air till transparent and post vulcanized at 100°C for 30 minutes in an air circulated oven. Fully vulcanized samples were then cooled and packed in sealed polyethylene bags for testing.

Aqueous dispersion of LS was added to the PUR latex stirred and cast as indicated above and air dried till transparent. Note that PUR has not been cured.

Latex blends with various PUR/NR ratios (viz. 1/1 and 8/2) with and without LS were produced in a similar way as described above.

Morphology detection. The dispersion of LS in the latex films was studied by X-ray diffraction (XRD) and transmission electron microscope (TEM). XRD spectra were obtained in transmission mode using Ni-filtered CuKα radiation (λ=0.1542nm) by a D500 difractometer (Siemens, Germany). The samples were scanned in step mode by 1.5°/min rate in the range of 2θ<12°. For comparison purpose the XRD spectrum of the LS powder was also registered, however, in reflection.

TEM images were taken in LEO 912 Omega microscope with an accelerator voltage of 120keV. Thin sections (ca. 100nm) of the specimens were cryo-cut with a diamond knife at ca. –120°C and used without staining.

In order to get a deeper insight in the possible interaction between LS and rubber Fourier transform infrared spectroscopic (FTIR) measurements were also done. FTIR on the films was performed in attenuated total reflection mode (ATR) at a resolution of 4cm^{-1} using a Nicolet P 510 spectrometer. LS powder was pressed with KBr powder for FTIR measurements in transmission mode.

Property assessment. Dynamic mechanical thermal analytic (DMTA) spectra of the films were recorded by an Eplexor 25N device (Gabo Qualimeter, Germany) in tension mode at 10Hz frequency. The complex elastic modulus, its constituents (viz. storage, E'and loss parts, E") along with the mechanical loss factor (tanδ) were determined as a function of the temperature (T = -100°C...+60°C). The static and dynamic tensile load applied were 2 and ±1N, respectively and the heating rate was set to 2°C/min.

Tensile tests to determine the ultimate properties (strength, elongation) along with the moduli at selected elongations were performed at room temperature (RT) on dumb-bells according to ASTM D 412 using 500mm/min crosshead speed . The tear strength at RT was determined according to ASTM D 624 using crescent shape specimens at a crosshead speed of 500mm/min. The tensile and tear properties were determined also after heat aging (storage for 7 days at 70°C).

RESULTS AND DISCUSSION

Morphology. Figure 1 shows the XRD spectra of the LS and the LS-containing films of various compositions. Note that the LS shows two smaller peaks in addition to the major one. These peaks correspond to the following interlayer distances based on the Bragg's equation: 1.22, 1.10 and 0.95nm. So the LS used contained some small fractions with higher intergallery distance than the bulk material. LS has been intercalated by NR in the related compound as the interlayer distance of the LS increased to 1.19nm -

1.31nm. The appearance of the related broad peak suggests that the degree of NR intercalation is different. A considerably better intercalation was noticed for the PUR latex where two peaks were resolved. The major peak indicates that the interlayer distance of the LS widened to 1.73nm from the initial 0.95nm. This effect can be assigned to the higher polarity of PUR compared to NR which favors the compatibility with LS. Similar to PUR the NR/PUR latex blend shows also two peaks. Albeit they appear at slightly higher interlayer distances than in PUR, these peaks are likely the same. The intensity ratio of these peaks is, however, opposed to that of the pure PUR nanocomposite. Before discussing this aspect attention should be paid to results achieved by TEM and FTIR.
TEM pictures in Figure 2 evidence the good intercalation of LS by PUR. One may get the impression that a part of LS has been even exfoliated. Pictures in Figure 2 demonstrate further the high aspect ratio of the LS. This is becoming obvious when the size of the flat-one laying platelets (disks) in Figure 2b are considered.

The dispersion of LS in PUR/NR (1/1) latex blend differs considerably from that of the PUR. TEM picture in Figure 3 show that NR and PUR are not compatible. Note that particles from the sulfur prevulcanized NR appear dark in these TEM images. Layered silicate stacks can be located at the boundary of the PUR (light) and NR (dark) phases. Pronounced intercallation and possible exfoliation took place only in the PUR phase - see Figure 3b. The silicate layers and aggregates cover the NR particles resulting in a skeleton (house of cards) structure. This peculiar morphology is rather specific for NR nanocomposites produced by the latex route if the length of the LS is commensurable with that of the rubber particle size in the latex. Based on the TEM results we can now explain the difference in the XRD spectra of the PUR and PUR/NR latices. Recall that LS is less intercalated by NR than by PUR. So, in the case of the PUR/NR blend, PUR should intercalate the double amount of LS due the volume excluded by NR. Bearing in mind that there is an optimum in the LS content in respect to intercalation/exfoliation phenomena, a substantial increase in the LS may cause its reaggregation (confinement). However, this does not yield necessarily a deterioration in the mechanical properties. Recall that the prevulcanized NR particles force the silicate aggregates in the neighbouring PUR phase to cover their surface. This results in a skeleton morphology as the length of the silicate layers is higher than those of the diameter of the particles (Figure 3). The formation of this skeleton structure may yield improved mechanical properties.

Interesting information can be derived from the FTIR analysis, too. Several attempts to characterise PUR/clay [12-14] or NR/clay [15-16] nanocomposites using FT-IR spectroscopy have already been made. In most of the cases just the verification of the incorporation of the clay into the matrix was the outcome. Differences between the spectra of unfilled material and nanocomposite were searched among peaks corresponding to vibrations of the macromolecular chains of either PUR or NR. Chen et al. [12] tried to estimate the degree of interaction between the silicate layers and the PUR segments evaluating the ratio of the absorption peaks of the hydrogen bonded and the free groups of NH or C=O. Recently, Loo et al. monitored the stress-induced peak shift in the Si-O stretching vibration of montmorillonite clay in nylon-6/nanoclay nanocomposite [17]. The vibration of the Si-O bond was found to be sensitive to stress showing a shift to lower wavenumbers with increasing level of strain.

The absorption bands in the infrared (IR) spectrum of various layered silicates depend on their chemical composition [18]. In case of fluorohectorite the IR spectrum presents mainly two peaks corresponding to the Si-O stretching vibration at the 1005 cm^{-1} and the Si-O bending vibration at the 476 cm^{-1} [13, 17, 18]. The sensitivity of these peaks to intercalation/exfoliation phenomena is an aspect observed in the current paper.

As presented in Figure 4, the Si-O stretching vibration at the 1005 cm^{-1} in the case of PUR/LS system is appearing as a shoulder around 990 cm^{-1} superposed to the 967 cm^{-1} peak of PUR. Moreover, the Si-O bending vibration at the 476 cm^{-1} is shifted to the 467 cm^{-1} presenting a clear peak due to the fact that at that region the PUR does not present any peak. Considering the fact that the PUR is capable of intercalating the layers of LS (i.e. TEM and WAXS experiment), the peak position is likely due to the interaction of the macromolecular chain with the silicate layers.

Figure 5 presents the spectra in the case of NR/LS system. The Si-O stretching vibration at the 1005 cm^{-1} and the Si-O bending vibration at the 476 cm^{-1} are shifted to 998 cm^{-1} and 470 cm^{-1} respectively. According the TEM and WAXS findings, the NR/LS system showed less significant intercalation (and thus layer expansion) than PUR. This means that the interaction between the NR macromolecular chains and the layered silicate is rather low. Respectively, the peak shift in the IR spectra for the NR/clay nanocomposite was also slighter than the shift for PUR/clay nanocomposite.

The spectra of the PUR/NR blend reinforced with LS is presented in Figure 6. The Si-O stretching vibration at the 1005 cm^{-1} and the Si-O bending vibration at the 476 cm^{-1} are shifted to 994 cm^{-1} and 468 cm^{-1} respectively. This means that there is a rather good intercalation of LS in the blend, similarly to the neat

PUR. Considering the TEM images, the component that worked as intercalant in the blend was the PUR rather than the NR.

Consulting the above mentioned results, it is clear that PUR has two favourable peaks in the case of the XRD spectra. This means that there are two favourable and possible distances between the layers of the silicate during intercalation. In the case of the spectra from the blend these two peaks are also appearing but with totally opposite intensity. The volume during the mixing of the materials (glass plates) was each time the same and PUR is obvious that intercalates much better than NR (XRD spectra). Considering that in the case of the blend the volume that possess the two components is the half that they were possess alone in the glass plate, excluded volume phenomena should be present (also restricted mobility of macromolecular chains). The LS is mainly in the PUR area (TEM images), so the amount of LS that should be intercalated by PUR is not actually 10phr but something less than 20phr. Having in mind that there is an optimum in LS content in order intercalation/exfoliation phenomena to take place (enhanced properties at low filler level) [1-19-20], the increase of LS content in the PUR area should act reversal to the phenomenon. The NR/LS system gives raise to a peak in the XRD spectra around 7 degrees. Thus, the main peak for the blend around 7 degrees is quite logical, presenting also a smooth peak around 4.5 degrees.

Thermomechanical properties. Figure 7 shows the course of the storage modulus (E', Figure 7a) and mechanical loss factor (tanδ, Figure 7b) as a function of temperature for the latices studied. Comparing the DMTA traces of the plain rubbers with that of the blend one can notice that PUR and NR are fully incompatible. This is based on the fact that no change in the related glass transition temperatures (T_g) occurs due to blending and the stiffness follows the composition at ratio. This finding is in harmony with TEM results. The nanoreinforcement proved to be very efficient below the T_g of the matrix (plain rubbers) and below the component with the higher T_g (blend rubbers), respectively. The stiffness of the plain rubbers was increased by 1200-1500MPa (depending on the temperature) owing to 10% LS. One can notice that the formation of a skeleton structure in NR and PUR/NR blend is as efficient as the markedly better intercalation, however, without skeleton structure in PUR. Figure 7b demonstrates that nanoreinforcement caused a dramatic decrease in the tanδ. This finding is in concert with the expectation: the molecular mobility is strongly hampered owing to the strong LS/rubber interactions. Note that in Figure 7a the major reason of blending NR with PUR is obvious: the blend exhibits a markedly higher stiffness than NR up to T≈10°C (T_g of PUR).

Tensile mechanical properties. Table 2 lists the mechanical properties of the rubbers and their nanocomposites before and after heat aging. Note that LS nanoreinforcement was very effective for PUR. The ultimate tensile strength as well as tear strength strongly increased (more than 3 times) and a dramatic improvement was found in the moduli at different elongations. As expected, the LS reinforcement strongly decreased the ultimate elongation. A similar scenario, however, with less improvement in the stiffness and strength was found for the NR. The most interesting results presented the PUR/NR (1/1 and 8/2) blend based nanocomposites due to their excellent mechanical performance. So, part of the expensive PUR latex can be replaced by inexpensive NR latex without sacrificing the mechanical response of the nanocomposites. A further advent of compounding NR with PUR is related to the aging of the latter. Heat aging of PUR accompanied with crosslinking (via interchange reactions) which enhances the stiffness and strength data of PUR, PUR-containing blend and related nanocomposites.

CONCLUSIONS

Based on this work devoted to study the morphology dependent mechanical properties of layered silicates (LS) reinforced NR-, PUR- and PUR/NR-blend based nanocomposites produced by the latex route, the following conclusions can be drawn:

- LS is more compatible and thus better intercalated by PUR than by NR. In the case of sulfur prevulcanized NR latex and its blends with PUR the LS forms a skeleton (house of cards) structure. The onset of this structure is favored by the prevulcanization of the NR. The reinforcing efficiency of the skeleton-type structure (NR) was comparable with that of composed of LS layers and stacks (PUR).
- Albeit PUR and NR are completely incompatible, the mechanical properties of the nanocomposites based on their blends (PUR/NR ratios 1/1 and 8/2) agreed with those of the plain PUR. The effect of LS dispersion (intercalation/exfoliation) was best reflected in stiffness- and strength- related characteristics.

REFERENCES

[1] Karger-Kocsis, J.; Wu, C.-M. Polym Eng Sci, submitted.

[2] Utracki, L. A.; Kamal, M. R. Arab J Sci Eng 2002, 27, 43.

[3] Pinnavaia, T. J.; Beall, G. W.; Eds. Polymer-clay nanocomposites; Wiley: New York, 2000.

[4] Varghese, S.; Karger-Kocsis, J. Polymer 2003, 44, 4921.

[5] Zhang, L.; Wang, Y.; Wang, Y.; Sui, Y.; Yu, D. J Appl Polym Sci 2000, 78, 1873.

[6] Wang, Y.; Zhang, L.; Tang, C.; Yu, D. J Appl Polym Sci 2000, 78, 1879.

[7] Wu, Y.-P.; Jia, Q.-X.; Yu, D.-S.; Zhang, L.-Q. J Appl Polym Sci 2003, 89, 3855.

[8] Wu, Y.-P.; Zhang, L.-Q.; Wang, Y.-Q.; Liang, Y.; Yu, D.-S. J Appl Polym Sci 2001, 82, 2842

[9] Cai, H.-H.; Li, S.-D.; Tian, G.-R.; Wang, H.-B.; Wang, J.-H. J Appl Polym Sci 2002, 87, 982.

[10] Stephen, R.; Raju, K. V. S. N.; Nair, S. V.; Varghese, S.; Oommen, Z.; Thomas, S. J Appl Polym Sci 2003, 88, 2639.

[11] Varghese, S.; Karger-Kocsis, J.; Gatos, K. G. Polymer 2003, 44, 3977.

[12] Chen, T. K.; Tien, Y.-I.; Wei, K.-H. Polymer 2000, 41, 1345.

[13] Zhang, X.; Xu, R.; Wu, Z.; Zhou, C. Polym Int 2003, 52, 790.

[14] Tien, Y. I.; Wei, K.-H. Polymer 2001, 42, 3213.

[15] Joly, S.; Garnaud, G.; Ollitrault, R.; Bokobza, L.; Mark, J. E. Chem Mater 2002, 14, 4202.

[16] Arroyo, M.; López-Manchado, M. A.; Herrero, B. Polymer 2003, 44, 2447.

[17] Loo, L, S.; Gleason K. K. Macromolecules 2003, 36, 2587.

[18] Mookherjee, M.; Redfern, S. A. T. Clay Minerals 2002, 37, 309.

[19] Alexandre, M.; Dubois, P.; Mater Sci Engng R 2000, 28, 1.

[20] Kim, J.-T.; Oh, T.-S.; Lee, D.-H. Polym Int 2003, 52, 1058.

Figure 1. XRD spectra of the layered silicate (LS) reinforced latex nanocomposites of various compositions

Note: for comparison purpose this figure contains the XRD spectrum of the LS (sodium fluorohectorite), as well

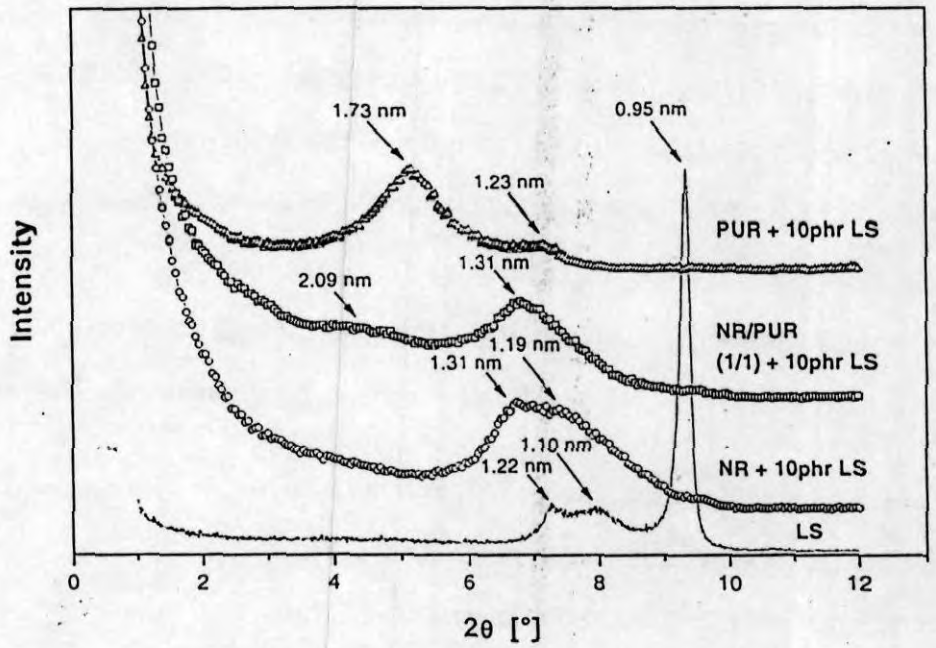

Figure 2a.

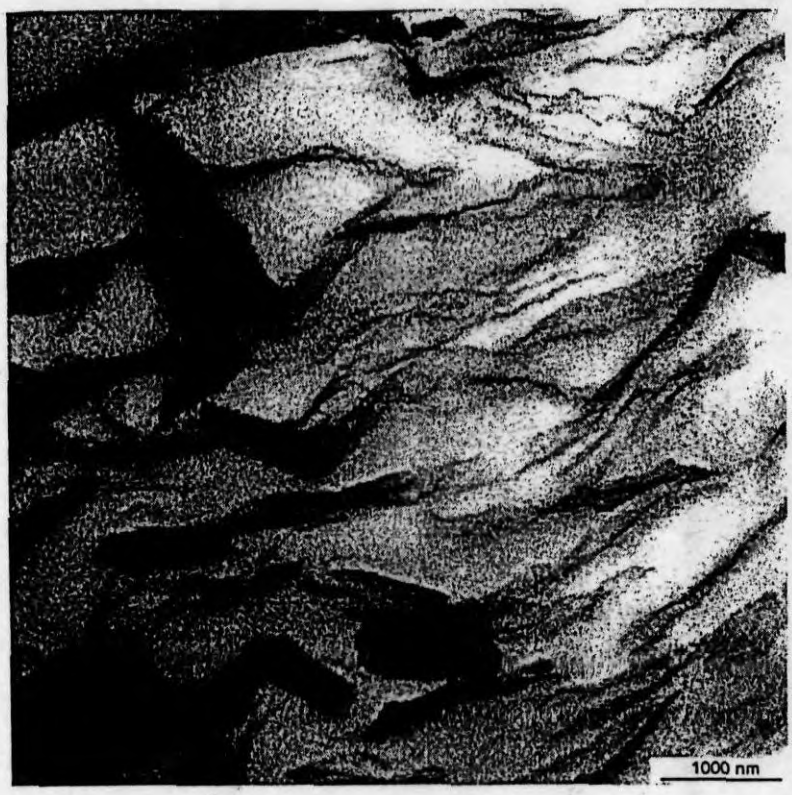

Figure 2b.

Figure 2. TEM images taken at various magnifications from the film cast of PUR latex containing 10phr LS

Figure 3a.

Figure 3b.

Figure 3. TEM pictures taken from the film cast of the PUR/NR (1/1) latex blend containing 10phr LS

Figure 4. FT-IR spectra of PUR, LS and PUR reinforced with LS 10phr

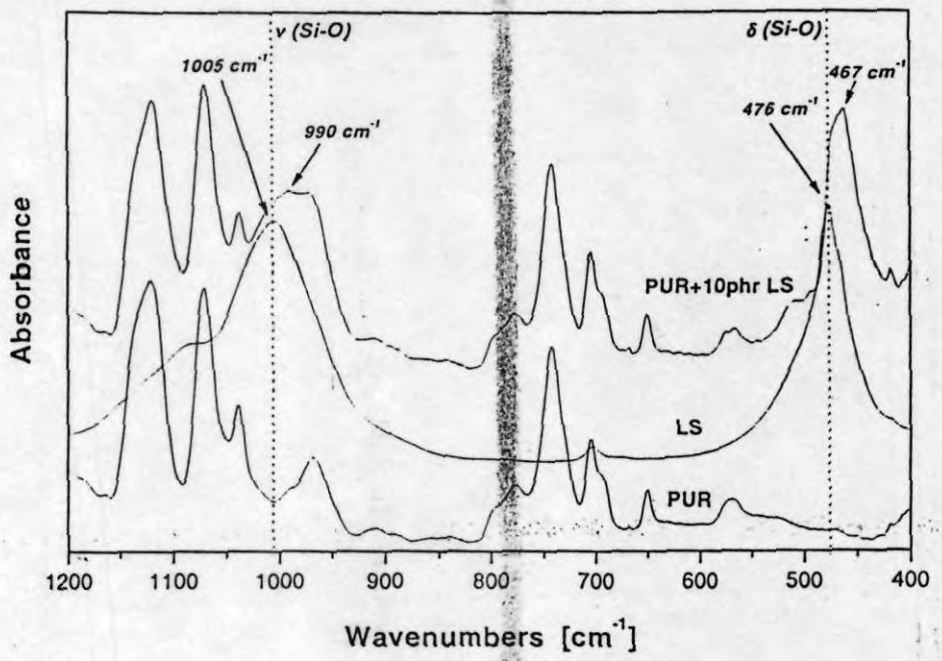

Figure 5. FT-IR spectra of NR, LS and NR reinforced with LS 10phr.

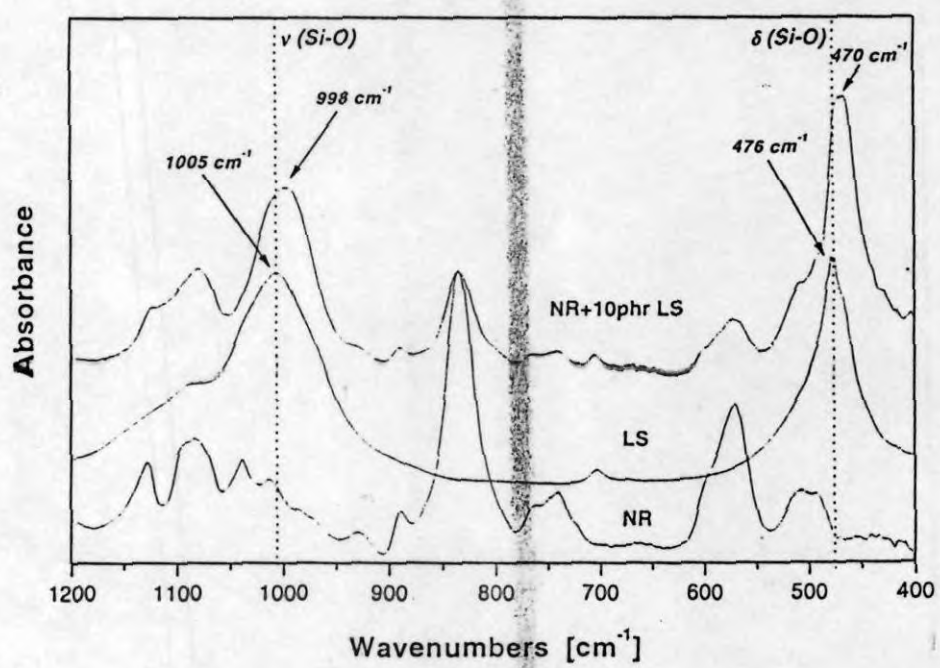

Figure 6. FT-IR spectra of PUR/NR (1/1) blend, LS and PUR/NR (1/1) blend reinforced with LS 10phr

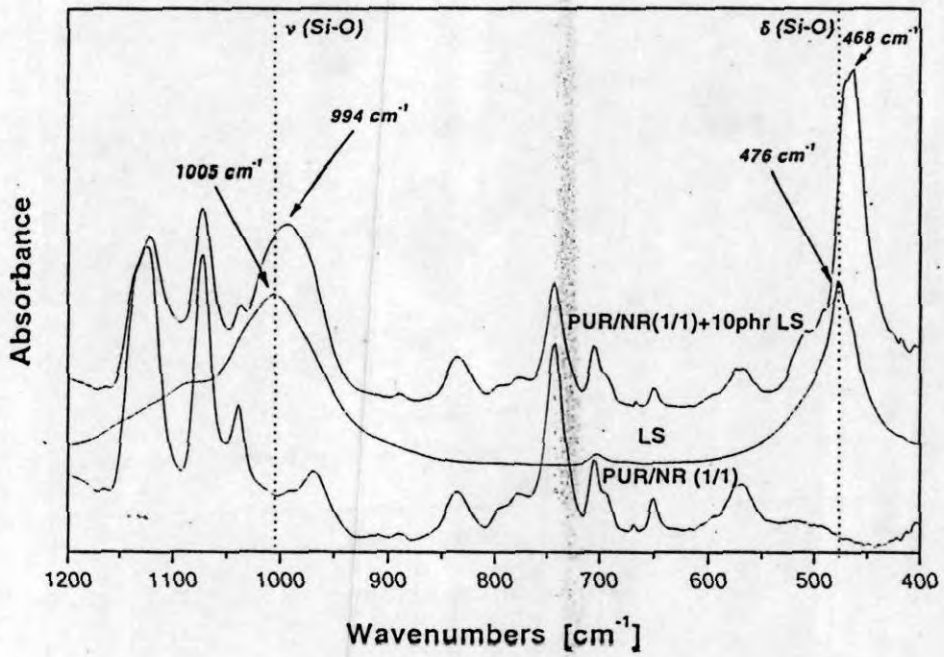

Figure 7a.

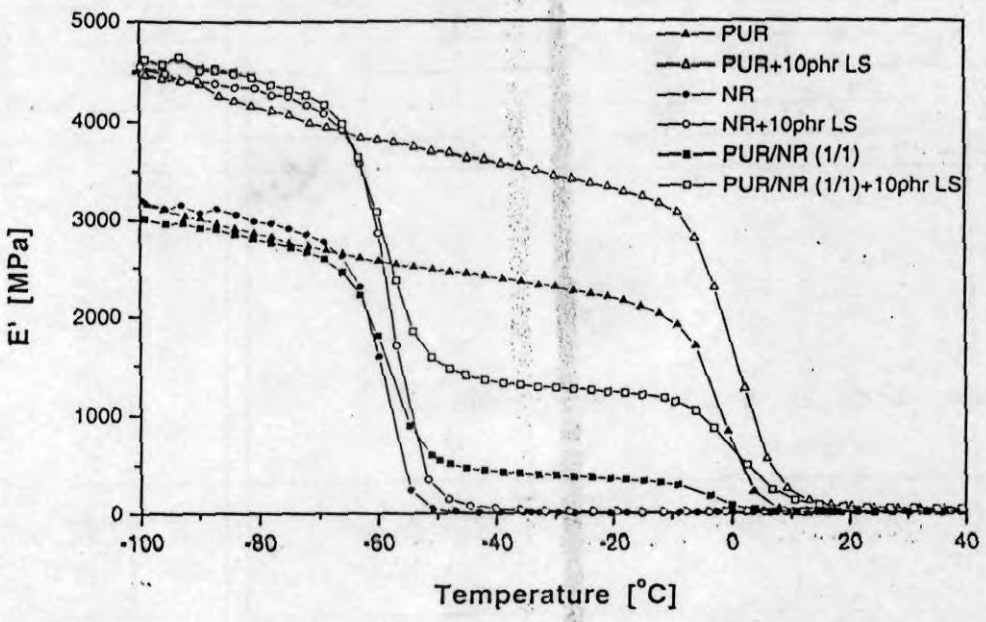

Figure 7b.

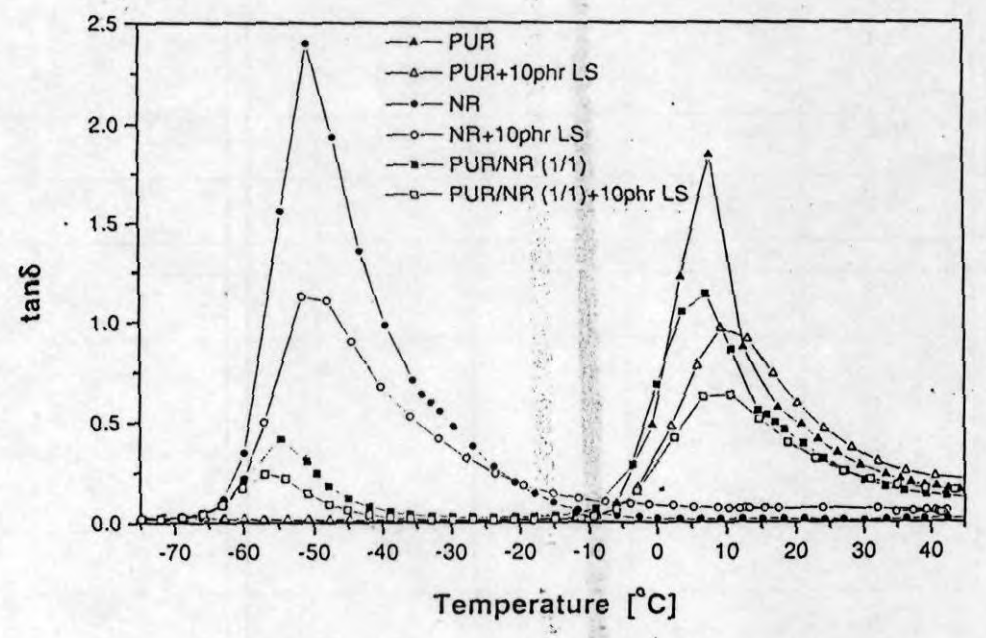

Figure 7. Storage modulus and mechanical loss factor as a function of temperature for pure and reinforced systems

Table 1. Formulation of NR prevulcanized latex. Designation: ZDMC is zincdimethyldithiocarbamate

	Formulation	
	wet	dry
NR latex (60%)	166.7	100.0
10% KOH solution	1.0	0.1
50% ZDMC dispersion	2.0	1.0
50% sulfur dispersion	2.0	1.0

Table 2. Mechanical properties of the rubber nanocomposites studied

	Before aging					
Property	PUR	PUR+LS 10phr	NR	NR+LS 10phr	PUR/NR (1/1) +LS 10phr	PUR/NR (8/2) +LS 10phr
Tensile strength (MPa)	4.0	15.9	19.6	23.5	12.4	11.4
Tensile modulus (MPa)						
100% Elong.	0.8	5.6	0.7	2.1	4.3	4.9
200% Elong.	0.9	7.8	0.9	3.1	5.9	6.7
300% Elong.	1.1	10.1	1.1	4.5	7.5	8.4
Elongation at break (%)	932	543	881	697	556	469
Tear strength (kN/m)	12.3	54.5	28.0	36.7	59.9	50.7
After aging at 70°C for 7 days						
Tensile strength (MPa)	10.5	17.9	20.8	23.5	16.7	17.5
Tensile modulus (MPa)						
100% Elong.	1.1	7.6	0.7	2.7	6.7	7.4
200% Elong	1.4	10.7	0.9	4.2	9.4	10.4
300% Elong.	1.8	13.5	1.1	6.0	11.6	13.0
Elongation at break (%)	772	444	768	620	484	447